Thermal convection in colloidal suspensions with negative separation ratio

Andrey Ryskin and Harald Pleiner
Max-Planck-Institut für Polymerforschung, D-55021 Mainz, Germany
(Received 31 August 2004; published 13 May 2005)

Thermal convection in colloidal suspensions of nanosized particles is investigated. Representative examples for such materials are ferrofluids, but since we do not imply any external magnetic field, the description applies to nonmagnetic suspensions as well. With the grain size being large on molecular length scales, the particle mobility is extremely small, allowing to disregard the concentration dynamics in most cases. However, due to the pronounced Soret effect of these materials in combination with a considerable solutal expansion, this cannot be done when thermal convection is under consideration. Here we consider the case when the separation ratio (the Soret coefficient) is negative. This case reveals a much richer variety of phenomena than that of positive separation ratio. In particular, for heating from below we find a linear oscillatory instability, whose amplitude, however, relaxes to zero on the long turn and is thus transient only and, at higher Rayleigh numbers, a finite amplitude stationary instability coexistent with the linearly stable convection-free state. By heating from above short-length-scale convective structures occur, whose wavelength depends on the Rayleigh number.

DOI: 10.1103/PhysRevE.71.056303 PACS number(s): 47.20.−k, 44.27.+g

I. INTRODUCTION

Thermal convection in binary mixtures has attracted much research activity in the past (see [1–3] for a review). In comparison to the pure fluid case, the dynamics and the bifurcation scenarios are more complicated due to the extra degree of freedom associated with the concentration field. Thereby solutal currents are not only driven by concentration gradients, they occur also in response to temperature inhomogeneities. This is denoted as the thermodiffusive or Soret effect. Its influence on the convective buoyancy force is quantified by the dimensionless separation ratio ψ.

When the thermal convection problem is considered in colloidal suspensions rather than in molecular binary mixtures, one has to take into account the very distinct time scales involved. The diffusion of colloidal particles is much slower than a typical molecular diffusion and the diffusion time is about two or three orders of magnitude smaller. This is reflected in the value of the Lewis number L, which in colloidal suspensions is $L\sim10^{-4}-10^{-5}$ compared to $L\sim0.1-0.01$ in molecular binary mixtures. In addition, the two constituents of a colloidal suspension (the solvent and the colloidal particles) have very different densities. For example, for ferrofluids with colloidal particles made of magnetite and dissolved in water the ratio of the two densities can be as large as ~5 [4]. As a result, there is a very high separation ratio in these materials. The combination of these two features (high ψ and low L) makes the consideration of the convection problem in ferrofluids different from molecular binary mixtures [5–7]. In particular, the experimentally relevant initial state of the concentration field is different from the linear profile usually considered.

In the following we phrase our discussion in terms of ferrofluids, since they are probably the most important application for our investigations and there are many measurements of material parameters available for ferrofluids [8–12]. In principle, this description is valid for nonmagnetic suspensions, too, as long as no external magnetic field is involved.

In two recent publications [5,6] we have discussed the thermal instability in ferrofluids with positive separation ratio, without and with an external magnetic field, respectively. However, the separation ratio of ferrofluids can be positive or negative [8] depending on the nature of the system. Usually, ferrofluids with steric stabilization possess positive separation ratio ψ, while for ferrofluids with electrostatic stabilization ψ is expected to be negative. Examples for the latter are maghemite and cobalt ferrite particles dissolved in water and stabilized by H^+ or citrate ions [8]. The value of ψ depends linearly on the concentration and can reach absolute values comparable to those of stericly stabilized similar ferrofluids [8], i.e., $|\psi|\sim100-1000$. The present paper is devoted to the study of thermal convection in ferrofluids with negative separation ratio without external magnetic fields.

The paper is organized as follows. In the following section the problem is set up along with the governing equations and boundary conditions. In Sec. III we present the linear stability analysis for two different cases—heating from below and from above—and in Sec. IV the nonlinear behavior of the system is considered, where we restrict ourselves, however, to 2-dimensional roll patterns, for simplicity. A summary concludes the exposition.

II. SETTING UP THE PROBLEM

Let us consider a laterally infinite horizontal layer of an incompressible ferrofluid (density ρ, kinematic viscosity ν) bounded by two rigid impermeable plates. The setup is heated from below or above with a temperature difference ΔT between the plates. In the present paper we do not consider magnetic field related effects, thus the evolution equations for non-magnetic binary mixtures can be adopted. Taking $C(\mathbf{r},t)$ as the concentration of the solid constituent of the suspension, the dimensionless equations for the Eulerian fields of velocity $\mathbf{v}(\mathbf{r},t)$, temperature $T(\mathbf{r},t)$, and $C(\mathbf{r},t)$ read in Boussinesq approximation [13–15] for negative ψ

$$\nabla\cdot\mathbf{v}=0, \tag{1}$$

$$\partial_t \mathbf{v} + \mathbf{v} \cdot \boldsymbol{\nabla}\, \mathbf{v} = -\ \boldsymbol{\nabla}\, W + \mathrm{Pr}\, \boldsymbol{\nabla}^2 \mathbf{v} + \mathrm{Pr}\, \mathrm{Ra}[(T - \overline{T}) + |\psi|(C - \overline{C})]\mathbf{e}_z, \tag{2}$$

$$\partial_t T + \mathbf{v} \cdot \boldsymbol{\nabla}\, T = \boldsymbol{\nabla}^2 T, \tag{3}$$

$$\partial_t C + \mathbf{v} \cdot \boldsymbol{\nabla}\, C = L(\boldsymbol{\nabla}^2 C + \boldsymbol{\nabla}^2 T). \tag{4}$$

Here we have scaled length by the layer thickness h, time by the characteristic heat diffusion time h^2/κ, temperature by ΔT, and the concentration by $(D_T/D_c)\Delta T$. The scale for the pressure W is $\kappa^2\rho/h^2$. Thereby κ, D_C, D_T are the coefficients for heat, concentration and thermodiffusion, respectively. The quantities $\overline{T}$ and $\overline{C}$ are reference values defined as the mean values for temperature and concentration. Apart from the Prandtl number $\mathrm{Pr} = \nu/\kappa$ and the Lewis number $L = D_c/\kappa$ there is a third dimensionless material parameter, the separation ratio $\psi = D_T\beta_c/(D_c\beta_T)$, where $\beta_T = -(1/\rho)\partial\rho/\partial T$ and $\beta_c = (1/\rho)\partial\rho/\partial c$ are the thermal and solutal expansion coefficient, respectively. The dimensionless Rayleigh number $\mathrm{Ra} = \beta_T g h^3 \Delta T/(\kappa\nu)$ is the control parameter measuring the strength of the thermal drive. In Eq. (3) we have suppressed the Dufour effect a (heat current driven by a concentration gradient), since it is significant in gas mixtures only.

In addition to the equations of motion boundary conditions are needed. Taking the bounding plates to be no-slip for the velocity, highly heat conducting, and impermeable for concentration currents we have at the upper $(z = 1/2)$ and the lower $(z = -1/2)$ plates

$$\mathbf{v}|_{z=\pm 1/2} = \mathbf{0}, \tag{5}$$

$$T|_{z=\pm 1/2} = \overline{T} \mp \frac{1}{2}, \tag{6}$$

$$(\partial_z C + \partial_z T)|_{z=\pm 1/2} = 0. \tag{7}$$

Equation (7) guarantees that a concentration current cannot penetrate the plates. Owing to the Soret effect the applied temperature difference enforces a finite concentration gradient at the boundaries. Equations (1)–(4) together with the boundary conditions (5)–(7) complete the system of hydrodynamic equations for the variables $\mathbf{v}, T, C$.

There are two essentially different regimes—heating from below $(\mathrm{Ra} > 0)$ and heating from above $(\mathrm{Ra} < 0)$. In the first case we have an instability due to the temperature buoyancy force while the concentration buoyancy stabilizes the system. This can be considered in some sense as an extension of the one component liquid convection with some additional effects due to the presence of the concentration buoyancy. In the second case the driving force for the instability is the buoyancy force due to the concentration field, while the thermal buoyancy is stabilizing. This case has no analog in a one component system.

In the following sections on linear and nonlinear stability analysis, we first present the relevant equations valid for both cases (heating from below or from above) as far as possible, but then discuss the results for the different regimes, separately.

III. LINEAR STABILITY ANALYSIS

A. Basic state and time scale separation

As shown in [5], the appropriate state to start the investigation of the convection instability in ferrofluids is a state where the temperature profile is fully developed while concentration just starts to build up the layers near the boundaries. This is due to the very different time scales of the concentration diffusion and heat conduction. So the initial state is given by

$$\mathbf{v} = 0, \tag{8}$$

$$T_{cond}(z) = \overline{T} - z, \tag{9}$$

for the velocity and the temperature field. For the concentration field we have a slowly developing profile given by the solution of the diffusion equation

$$\partial_t C_0 = L\partial_z^2 C_0 \tag{10}$$

with the inhomogeneous boundary condition

$$\partial_z C_0|_{z=\pm 1/2} = 1, \tag{11}$$

according to Eqs. (7) and (9). On the creeping time scale of the evolution of $C_0(z,t)$, $\tau \equiv Lt$, Eqs. (10) and (11) are valid for $\tau \geqslant L \simeq 10^{-4}$. An exact solution of Eqs. (10) and (11) can be found, for example, in [5].

B. Linear deviations

To probe the stability of the ground state, deviations are added whose time evolution is investigated. To that end we impose [16]

$$C(\mathbf{r},t) = C_0(z,t) + c(\mathbf{r},t), \tag{12}$$

$$T(\mathbf{r},t) = T_{cond}(z) + \theta(\mathbf{r},t), \tag{13}$$

and a nonzero velocity field $\mathbf{v}(\mathbf{r},t)$, whose z component is $w(\mathbf{r},t)$. Linearizing the equations of motion for the convective perturbations of the form $\theta, c, w \propto e^{\lambda t}\cos kx$ yields

$$\lambda(\partial_z^2 - k^2)w = -\ \mathrm{Pr}\,\mathrm{Ra}\ k^2(\theta + |\psi|c) + \mathrm{Pr}(\partial_z^2 - k^2)^2 w, \tag{14}$$

$$\lambda\theta - w = (\partial_z^2 - k^2)\theta, \tag{15}$$

$$\lambda c + w\partial_z C_0 = L(\partial_z^2 - k^2)(c + \theta). \tag{16}$$

The boundary conditions read

$$w|_{z=\pm 1/2} = 0, \tag{17}$$

$$\partial_z w|_{z=\pm 1/2} = 0, \tag{18}$$

$$\theta|_{z=\pm 1/2} = 0, \tag{19}$$

$$(\partial_z c + \partial_z \theta)|_{z=\pm 1/2} = 0. \tag{20}$$

Note that this system of ordinary differential equations is not autonomous, since $C_0(z,t)$ involves an explicit z and time dependence. But, as it is shown in [5], one can take C_0 = const. or $\partial_z C_0 = 0$ (uniform concentration distribution) for a simplified analytical treatment. However, the discussion in [5] also reveals that a linear stability theory, suitable to compare with a convection experiment, has to be based on the growth rates of the convective perturbations rather than on the threshold value for the temperature gradient.

C. Linear growth rate for the case Ra > 0

For the case Ra > 0 we assume that the spatial profiles of the velocity and the temperature are only slightly disturbed by the concentration dynamics. Accordingly, we represent their dependencies in terms of simple trigonometric test functions of a form that automatically fulfills the boundary conditions (17)–(19)

$$w(x,z,t) = A(t)\cos(kx)\cos^2(\pi z), \tag{21}$$

$$\theta(x,z,t) = B(t)\cos(kx)\cos(\pi z). \tag{22}$$

In contrast, for the convective concentration field c we allow for a steep boundary layer behavior, which we account for by the following multimode expansion:

$$c(x,z,t) = -\theta(x,z,t) + \cos(kx)\sum_{n=0}^{n=\infty} b_n(t)\cos(2\pi n z). \tag{23}$$

For $\lambda \gg L^{1/3}$ and $|\psi| \gg 1$ and with the approximation $k \approx \pi$ an analytical expression for λ as an implicit function of the control (Ra) and the material parameters (ψ, L, Pr) is obtained from Eqs. (14)–(16) and (21)–(23) [5]

$$3\mathrm{Ra}\,\mathrm{Pr}(\lambda - 2\pi^2 L|\psi|) = \lambda(2\pi^2 + \lambda)(27\pi^2\,\mathrm{Pr} + 7\lambda). \tag{24}$$

Without these approximations results are obtained numerically and shown in Fig. 1 and Fig. 2 illustrating the dependence of Re(λ) and Im(λ) on the reduced Rayleigh number $\varepsilon = \mathrm{Ra}/\mathrm{Ra}_c^0 - 1$ for the separation ratio $\psi = -10$. The dashed straight line bifurcating at $\varepsilon = 0$ indicates the reference case of a single-fluid convection.

For the case of a negative separation ratio the bifurcation takes place at the same point as for the single-fluid case. But in the present case there is a Hopf bifurcation at onset. When ε is increased the oscillatory frequency decreases and at the point $\varepsilon \approx 0.05$ the (linear) oscillatory instability becomes a stationary one. Above that point there are two bifurcation branches, of which only the most unstable is relevant, the upper branch (full line) in Fig. 1. If we increase ε further, this upper branch approaches asymptotically the bifurcation line of the single component liquid case ($\psi = 0$).

To understand this behavior, it should be noted that the initial state, whose stability is investigated, is one with an almost homogenous concentration profile. Since in the case of negative ψ the buoyancy force due to the concentration field is stabilizing, the state with a fully developed (linear) concentration profile is stable. Taking into account that the concentration profile develops in time there is the possibility that the nonconvective state becomes stable, again. On the other hand, the convective motion remixes the concentration field, making it almost homogeneous and, thus, leaves the system unstable. So the final state depends on the interplay of these two effects—the concentration field evolution due to the Soret effect, and the remixing of the concentration field due to convection. To make a prediction of the final state of this convection problem, one needs to solve the nonlinear problem. This is done in Sec. IV.

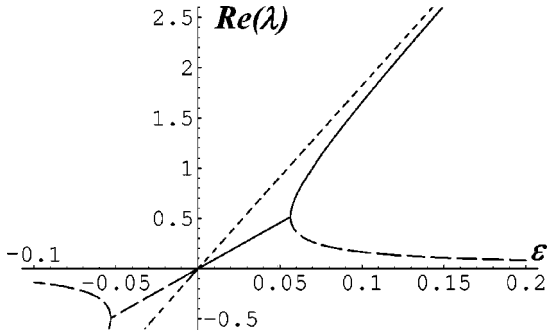

FIG. 1. The linear growth rate Re($\lambda(\varepsilon)$) for convective perturbations as a function of the reduced Rayleigh number $\varepsilon = \mathrm{Ra}/\mathrm{Ra}_c^0 - 1$. Here Ra_c^0 is the threshold for the onset of convection in a single-component fluid as shown by the dashed straight line (within the present Galerkin approximation $\mathrm{Ra}_c^0 = 1752$). Full lines indicate growth rates of unstable (or most unstable) modes. The parameters are $\psi = -10$, Pr = 7, and $L = 7 \times 10^{-4}$.

D. Linear growth rate for the case Ra < 0

Heating the system from above (Ra < 0) while $\psi < 0$ one is tempted to use a similar linear stability analysis as for Ra > 0 and $\psi > 0$ resulting in a threshold value [14]

$$\mathrm{Ra}_c = \frac{-1}{1+|\psi|}\mathrm{Ra}_c^0, \tag{25}$$

with $\mathrm{Ra}_c^0 = 1708$. Since the (linear) growth rate λ of the most unstable modes is very small near the threshold, we consider the range $\mathrm{Ra} \approx -\mathrm{Ra}_c^0$ where convection can be observed ex-

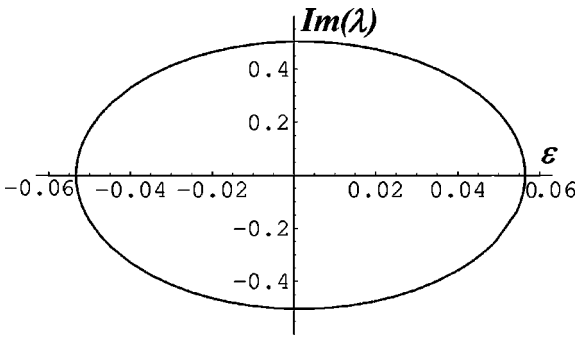

FIG. 2. The frequency of the oscillations Im($\lambda(\varepsilon)$) for convective perturbations as a function of the reduced Rayleigh number $\varepsilon = \mathrm{Ra}/\mathrm{Ra}_c^0 - 1$; parameters as in Fig. 1.

perimentally. However, since $|\psi| \gg 1$ for typical ferrofluids, we cannot use the result (24) for λ, because the assumption $k_c \approx \pi$ that holds in the case $\mathrm{Ra} > 0$ does not hold for the case $\mathrm{Ra} < 0$. The critical wave number depends on Ra sensitively so we need to find k_c for each value of Ra. The asymptotic behavior for large negative Ra can easily be found (cf. Appendix) almost independently of the special form of the Galerkin profiles (21)–(23), with the result

$$k_c^4 = \alpha |\mathrm{Ra}|, \tag{26}$$

where α is given by

$$\alpha = -\frac{|\psi|+2}{2} + \sqrt{\frac{(|\psi|+2)^2}{4} - 1 + |\psi|} \approx 1 \quad \text{for} \quad |\psi| \gg 1. \tag{27}$$

To this (asymptotic) wave number belongs the maximum (asymptotic) linear growth rate

$$\lambda = L\sqrt{\alpha|\mathrm{Ra}|}\frac{|\psi| - \alpha - 1}{1+\alpha} \approx \frac{L}{2}|\psi|\sqrt{|\mathrm{Ra}|} \quad \text{for} \quad |\psi| \gg 1. \tag{28}$$

These asymptotic relations are valid for $\sqrt{\alpha|\mathrm{Ra}|} \gg \pi^2$.

The physical reason why the wavelength of the most unstable mode becomes shorter and shorter when increasing the Rayleigh number, can be understood as follows. There are two buoyancy forces in the system—solutal and thermal buoyancy. The thermal buoyancy is stabilizing, while the solutal buoyancy is responsible for the instability. The diffusion of the temperature field is large compared to the concentration diffusion. Thus, short scale convective structures smooth out the temperature, while the concentration field follows the short scale structures due to the small diffusion. As a consequence, the thermal buoyancy cannot overcome the destabilizing solutal buoyancy, in particular for small wavelength fluctuations. If the thermal buoyancy increases, the critical wavelength has to decrease. Indeed, the tendency to shorter wavelengths for larger Rayleigh numbers has been observed in experiments [17,18].

We should note, however, that the linear stability analysis of a homogeneous concentration profile is relevant only, if the growth rate of the most unstable mode is larger than the evolution rate of the concentration profile, e.g., for $\lambda \gg L^{1/3}$ [5]. This is easily fulfilled for positive Ra (at $\mathrm{Ra} \approx \mathrm{Ra}_c^0$), but in the case $\mathrm{Ra} < 0$ the growth rate is $\sim L\sqrt{|\mathrm{Ra}|}$ [cf. Eq. (28)] and large enough to fulfill $\lambda \gg L^{1/3}$ for very large Rayleigh numbers, only. Thus, when the linear stability analysis given above is relevant, the use of the asymptotic relation (26) is possible. On the other hand, when the growth rate (or $|\mathrm{Ra}|$) is not large enough, we need to consider the evolution of the concentration profile C_0 and the growth of the perturbation simultaneously, in which case we are not able anymore to make the time scale separation and to describe the linear behavior of our system in terms of growth rates.

IV. NONLINEAR BEHAVIOR

A. Time evolution and numerical solution

To investigate the nonlinear behavior of the system we use numerical methods described in [5]. To that end we make the following ansatz of a 2-dimensional pattern, which is laterally (in x direction) periodic with wave number k

$$C(x,z,t) = C_0(z,t) + c_1(z,t)\cos kx, \tag{29}$$

$$T(x,z,t) = \theta_0(z,t) + \theta_1(z,t)\cos kx, \tag{30}$$

$$w(x,z,t) = w_1(z,t)\cos kx, \tag{31}$$

with the x component of the velocity $v_x(x,z,t) = -(1/k)\partial_z w_1(z,t)\sin kx$ due to the incompressibility condition. We have chosen this convective roll pattern for simplicity. Although other patterns (e.g., square patterns) seem to be possible [19], we do not think that the results are qualitatively different for different convection patterns. Substituting (29)–(31) into the nonlinear equations of motion (2)–(4) and sorting for different lateral dependencies yields the following system of equations,

$$\frac{1}{\mathrm{Pr}}\partial_t(\partial_z^2 - k^2)w_1 = (D^2 - k^2)^2 w_1 - \mathrm{Ra}\, k^2(\theta_1 - \psi c_1), \tag{32}$$

$$\partial_t C_0 + \frac{1}{2}\partial_z(w_1 c_1) = L\partial_z^2(C_0 + \theta_0), \tag{33}$$

$$\partial_t c_1 + w_1\partial_z C_0 = L(\partial_z^2 - k^2)(c_1 + \theta_1), \tag{34}$$

$$\partial_t \theta_0 + \frac{1}{2}\partial_z(w_1\theta_1) = \partial_z^2\theta_0, \tag{35}$$

$$\partial_t \theta_1 - w_1 + w_1\partial_z\theta_0 = (\partial_z^2 - k^2)\theta_1, \tag{36}$$

with the boundary conditions

$$\partial_z(c_1 + \theta_1)|_{z=\pm 1/2} = 0, \tag{37}$$

$$\partial_z(C_0 + \theta_0)|_{z=\pm 1/2} = 1, \tag{38}$$

$$\theta_1|_{z=\pm 1/2} = \theta_0|_{z=\pm 1/2} = 0, \tag{39}$$

$$w_1|_{z=\pm 1/2} = \partial_z w_1|_{z=\pm 1/2} = 0. \tag{40}$$

To solve this boundary-value problem we adopt vertical profiles w_1, θ_0, θ_1, C_0, and c_1 of the form

$$w_1(z,t) = A(t)\cos^2(\pi z), \tag{41}$$

$$\theta_1(z,t) = B(t)\cos \pi z, \tag{42}$$

$$\theta_0(z,t) = F(t)\sin 2\pi z, \tag{43}$$

$$C_0(z,t) = z - \theta_0(z,t) + \sum_{n=0}^{n=N} a_n(t)\sin(2n+1)\pi z, \tag{44}$$

$$c_1(z,t) = -\theta_1(z,t) + \sum_{n=0}^{n=N} b_n(t)\cos 2n\pi z, \qquad (45)$$

which satisfy the boundary conditions (37)–(40) identically. These equations describe a two-dimensional convective flow in the form of parallel rolls along the y axis in an infinite slab of thickness 1. We point out that for $\psi=0$ the concentration fields decouple from the temperature and the velocity pattern. This reduces Eqs. (41)–(43) to the 3-mode model introduced by Lorenz [20] to model the dynamics of convective rolls in a single-component Rayleigh-Bénard convection. For a non-zero ψ, the convection pattern is modified by the concentration field, but we can keep the single mode expansions for temperature and velocity without modifications, because the diffusivities for heat and momentum are large enough to prevent the appearance of strong gradients. By way of contrast, owing to the small Lewis number, the concentration field does build up steep boundary layers, which we account for by the multimode Fourier series given in (44) and (45). For C_0 the modes are antisymmetric in z and resemble the solution of the diffusion equation without advection [cf., e.g., Eq. (13) in [5]], while for c_1 symmetric modes are appropriate. The number N of contributing modes was taken large enough to ensure the results to be insensitive against a further increase of N. For the parameter values considered here, $N=50$ turned out to be sufficient to get the correct time evolution picture.

The equations for the mode amplitudes A, B, F, a_n, b_n are solved by a Runge-Kutta integration. The wave number k, usually taken to be the mode of maximum linear growth rate $\lambda(k,\mathrm{Ra})$, varies between 3 and 3.5 within the investigated Rayleigh number regime for the case $\mathrm{Ra}>0$, while for $\mathrm{Ra}<0$ we need to find k for each value of Ra, separately. For $\mathrm{Ra}>0$ the final predictions of our model do not depend sensitively on the k value chosen and we adopt in all our simulations $k=\pi$. All runs are started from an initial configuration characterized by an undisturbed linear temperature profile $T=T_{cond}$, a uniform concentration distribution $\partial_z C_0=c_1=0$, and small random velocity fluctuations.

B. The case Ra>0

According to the linear stability analysis (Sec. III C) there is an oscillatory instability in the interval of $0\leqslant\varepsilon\lesssim 0.05$. The typical simulation run for this regime is shown in Fig. 3. First, there is indeed an oscillating convective flow with an exponential increase of the envelope amplitude. However, the oscillation frequency increases with time indicating that the linear stability analysis does no longer apply. This increase of the frequency is a result of the growth of the concentration profile that piles up slowly with time. After some time ($\sim$40) the envelope amplitude of the oscillating flow pattern starts to decrease and is eventually damped out completely. This, again, is a result of the evolving concentration field that increases the stabilizing solutal buoyancy force to the extent that the system becomes stable again. The maximum amplitude that is reached is about one or two orders of magnitude larger than the initial value of the perturbation, while the time, at which that happens, is fairly independent of the initial value of the perturbations (at least if they are small).

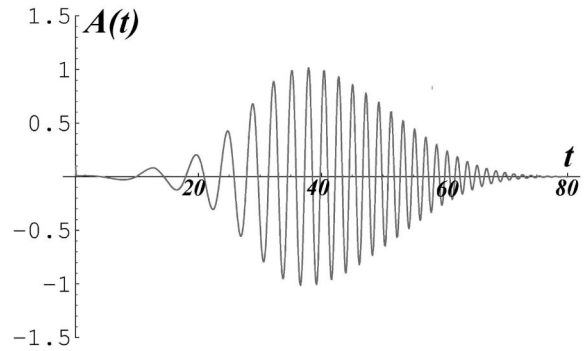

FIG. 3. The time dependence of the velocity amplitude $A(t)$ in the linear oscillatory instability regime ($\varepsilon=\mathrm{Ra}/\mathrm{Ra}_c^0-1=0.025$) in terms of the thermal diffusion time ($\psi=-10$, $\mathrm{Pr}=7$, and $L=7\times10^{-5}$).

For the regime of stationary instability $\varepsilon\gtrsim 0.05$, the time evolution of the velocity amplitude $A(t)$ is presented in Fig. 4 for two typical simulation runs. There are two different time evolution behaviors, depending on the initial value of the amplitude $A(0)$. The oscillating curve (S) in Fig. 4 corresponds to a small initial value $A(0)=10^{-5}$, while for the curve (L) with a large initial $A(0)=10^{-2}$ a stationary state with finite amplitude is obtained. If one waits long enough, the oscillations (S) die out and the case with no convection is reached again. Thus there are two stationary states—the quiescent initial state and a stationary convective one. The bifurcation into the latter is possible by finite amplitude perturbations only.

The explanation of the presence of these two stationary states is straightforward. When the concentration profile is fully developed the state without any convective motion is stable, since for negative ψ the concentration gradient is stabilizing. When the concentration field is homogeneous, the convection-free state is unstable. When we start from an initially homogeneous concentration distribution, the concentration profile builds up together with the development of the

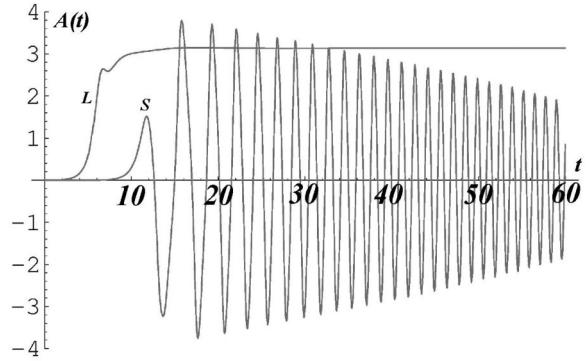

FIG. 4. Same as Fig. 3, but in the stationary instability regime ($\varepsilon=\mathrm{Ra}/\mathrm{Ra}_c^0-1=0.085$) for large ($L$) and small ($S$) initial perturbation amplitudes.

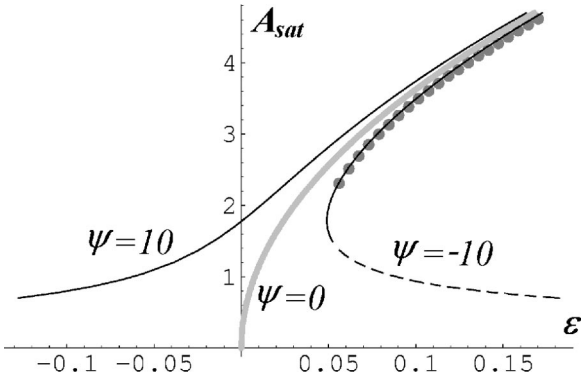

FIG. 5. The saturation amplitude $A_{sat}=A(t\to\infty)$ as a function of $\varepsilon=\mathrm{Ra}/\mathrm{Ra}_c^0-1$ (parameters as in Fig. 3). The gray thick line corresponds to a single-component fluid ($\psi=0$). The gray dots show numerical solutions, while the solid lines are analytical solutions for $\psi=-10$ [Eq. (46)] and $\psi=10$ [5]. The dashed curve indicates an unstable solution.

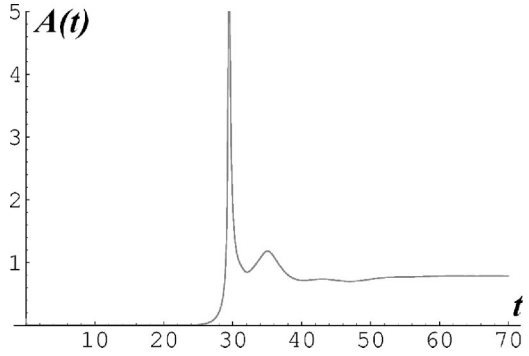

FIG. 6. The time dependence of the convection amplitude $A(t)$ by heating from above ($\mathrm{Ra}=-129983$); parameters as in Fig. 3.

instability. If the convective motion is already strong enough (by starting with a finite convection amplitude), it can stop the development of the concentration profile by advection. So the decisive point is, whether the convective motion becomes strong enough to stop the buildup of the concentration profile, or whether the concentration field has enough time to build up its linear profile that stops convective motion. The time of the instability evolution depends logarithmically on the initial amplitude of the perturbation. Thus, the final state that is reached depends on the initial value of the perturbation amplitude.

The saturation amplitude of the stationary convective state can also be obtained analytically. In [6] we derived an analytical formula [Eq. (83)] for the saturation amplitude for the case of a positive separation ratio in the presence of a magnetic field. This formula is valid for negative ψ as well and is adjusted to the present field-free case by $M_1=0=M_2$. It can be written as

$$\frac{18\pi^4}{\mathrm{Ra}}=\frac{1}{1+\dfrac{3}{40\pi^2}A^2}-\frac{32\pi^2}{3A^2}L|\psi|. \tag{46}$$

A similar formula has been derived in [16] (Eq. 4.1b) using a 5 mode Galerkin representation of the concentration field. The bifurcation scenario is discussed using the amplitude A of the convective flow as a function of the Rayleigh number (Fig. 5). There are two branches, one branch (solid line) approaches the reference curve for pure liquids, while the other branch (dashed line) goes asymptotically to a small value $\sim\sqrt{L|\psi|}$ for large Ra. According to our numerical solutions only the upper branch corresponds to a stable solution and can be realized experimentally.

C. The case $\mathrm{Ra}<0$

When heating from above we need to determine the wave number k_c of the most unstable mode for each value of the Rayleigh number before we can solve the nonlinear problem. As it was noted in Sec. III D, we can reliably use the linear stability analysis only for large values of $|\mathrm{Ra}|$, where $k_c^4\sim|\mathrm{Ra}|$. A typical simulation run for heating from above is given in Fig. 6. Before the amplitude takes its stationary value there is an overshoot, which is also observed in experiments [17,18]. The convection amplitude always saturates to a finite value, independently of the initial conditions and the k_c value chosen. For moderate values of the Rayleigh number ($|\mathrm{Ra}|\sim\pi^4$), we cannot predict the wavelength of the structure that is actually realized, but from the numerical simulations we can infer that, qualitatively, the behavior of the system is independent of the wavelength.

To find the saturation amplitude as a function of the Rayleigh number we cannot use the formula (46) since in that formula we have already fixed $k=\pi$. If we repeat the procedure in [6] that led to (46) for an arbitrary value of k, we get the general expression

$$\frac{3k^4+8k^2\pi^2+16\pi^4}{4k^2|\mathrm{Ra}|}=\frac{-15}{3A^2+20(k^2+\pi^2)}+\frac{4L|\psi|}{A^2}. \tag{47}$$

As discussed in Sec. III D our treatment is applicable for large values of $|\mathrm{Ra}|$, only, in the case of negative ψ and negative Ra. In that regime we can use Eq. (26) for the value of k_c and get the saturation amplitude

$$A^2\simeq\frac{16}{3(1+\alpha)}L|\psi|\sqrt{\alpha|\mathrm{Ra}|}. \tag{48}$$

In Fig. 7 this asymptotic expression (48) is shown as a solid line. Equation (48) also reveals that this instability is not of the standard pitchfork variety, since A scales with $|\mathrm{Ra}|^{1/4}$ rather than $|\mathrm{Ra}|^{1/2}$. One should keep in mind, however, that Eq. (48) is valid for $|\mathrm{Ra}|\gg|\mathrm{Ra}_c|$, Eq. (25), only, and does not determine the possible form of an amplitude equation close to onset. The unusual scaling of the pattern amplitude in the experimentally relevant regime far above $|\mathrm{Ra}_c|$ is a consequence of the Ra dependence of the appropriate wavelength. Close to onset such a feature would be quite uncommon. Here, it is based on the huge difference between the concentration and the thermal diffusion time scales, as discussed after Eq. (28).

V. SUMMARY

When heating from below any binary mixture with negative separation ratio, the thermal and solutal density gradi-

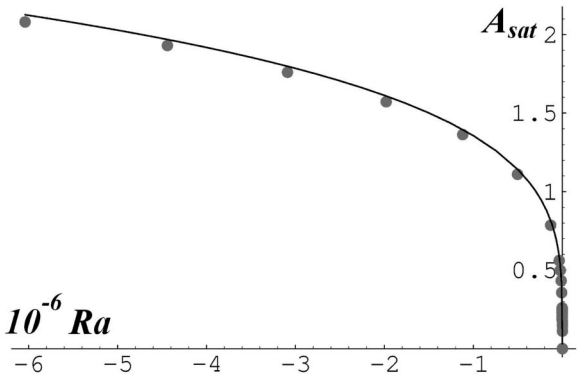

FIG. 7. The saturation amplitude A_{sat} of the convective velocity by heating from above as a function of the Rayleigh number times 10^{-6}. Gray dots are numerical solutions, while the solid line is the analytical solution (48); parameters as in Fig. 3.

ents are opposed such that the linear stationary thermal instability is suppressed for $\psi<-1$. Instead, this antagonistic behavior leads to a linear convective instability of the oscillatory type at Ra_c^0, the critical Rayleigh number for the onset of convection in the single fluid case. This feature is found for ferrofluids, too, but the nonlinear treatment shows that the linearly unstable oscillatory states are transients only and decay after some time, rendering the final convection-free state stable. Above a second threshold, somewhat higher than Ra_c^0, a finite amplitude stationary instability is found, while small amplitude disturbances do not destroy the convection-free state.

When heating from above any binary mixture with negative separation ratio $\psi<-1$, a linear stationary instability is found, which is basically driven by the solutal buoyancy and only slightly modified by thermal variations. In ferrofluids, however, the concentration and temperature dynamics show completely different behavior. Thus, this stationary instability (by heating from above and negative separation ratio) is very different from that obtained by heating from below with a positive separation ratio. In the former case small scale structures arise at very high Ra numbers, whose wavelength decreases strongly with increasing Ra. For smaller Ra numbers ($|\mathrm{Ra}|\sim \mathrm{Ra}_c^0$) the present procedure, using the separation of thermal conduction and concentration diffusion times, breaks down.

ACKNOWLEDGMENTS

Helpful discussions with M. Lücke are gratefully acknowledged. This work is supported by the Deutsche Forschungsgemeinschaft through SPP 1104, magnetic colloidal fluids.

APPENDIX

In this appendix we derive the asymptotic relations (26)–(28). To that end we use the Galerkin representation (21)–(23) and get the (negative) Rayleigh number Ra, as a function of the wave vector k and the growth rate λ

$$-|\mathrm{Ra}| = \frac{(k^2+\pi^2)(3k^4+8k^2\pi^2+16\pi^4)(Lk^2+\lambda)(Lk^2+L\pi^2+\lambda)}{3k^2(k^4L^2[1+\psi]+Lk^2(4L\pi^2[1+\psi]+\lambda[2+\psi])+\lambda(\lambda+L\pi^2[4+\psi]))}. \tag{A1}$$

Here we have simplified the formula using the fact $\lambda \ll \pi^2\mathrm{Pr}$. If we consider relation (A1) as an implicit function $\lambda(\mathrm{Ra},k)$, we obtain the wavelength of the most unstable mode by finding the maximum of this function with respect to k for a given value of Ra. Analytically this procedure is rather cumbersome, but it reveals rigorously that λ scales with Lk^2 and is, thus, rather small. The numerical maximization of $\lambda(\mathrm{Ra},k)$ shows that k grows when Ra increases. For large values of k ($\gg\pi$) we can simplify formula (A1) and get

$$\frac{k^2}{|\mathrm{Ra}|} = \frac{-1}{k^2} + \frac{|\psi|L}{\lambda+Lk^2}. \tag{A2}$$

for negative ψ and negative Ra. If we fix Ra and consider λ as a function of k, this function has a maximum given by (26), which corresponds to the most unstable mode. The wave number of the most unstable mode and the growth rate for this mode are given by (28).

A simpler way of getting the asymptotic relations (26)–(28) that also reveals the physical nature of this case, is to consider Eqs. (14)–(16) far from the upper and lower boundaries. In this region the fields are rather smooth. Due to the smallness of $\lambda\sim Lk^2$ we can neglect the terms containing the growth rate λ anywhere, except for the equation for the concentration field and get

$$0 = -\mathrm{Ra}\, k^2(\theta-\psi c)+k^4 w, \tag{A3}$$

$$w = k^2\theta, \tag{A4}$$

$$\lambda c = -Lk^2(c+\theta). \tag{A5}$$

Thus we have reduced the differential equations to algebraic ones. That means that the dispersion relation decouples from the problem of finding the field profiles. The condition to have a nontrivial solution of (A3)–(A5), is identical to Eq. (A2).

[1] J. K. Platten and J. C. Legros, *Convection in Liquids* (Springer, Berlin, 1984).
[2] M. C. Cross and P. C. Hohenberg, Rev. Mod. Phys. **49**, 581 (1993).
[3] M. Lücke, W. Barten, P. Büchel, C. Fütterer, St. Hollinger, and Ch. Jung, in *Evolution of Spontaneous Structures in Continuous Systems*, edited by F. H. Busse and S. C. Müller, Lecture Notes in Physics, Vol. 55 (Springer, Berlin, 1998), p. 127.
[4] R. E. Rosensweig, *Ferrohydrodynamics* (Cambridge University Press, Cambridge, England, 1985).
[5] A. Ryskin, H.-W. Müller, and H. Pleiner, Phys. Rev. E **67**, 046302 (2003).
[6] A. Ryskin and H. Pleiner, Phys. Rev. E **69**, 046301 (2004).
[7] M. I. Shliomis and M. Souhar, Europhys. Lett. **49**, 55 (2000).
[8] J. Lenglet, A. Bourdon, J.-C. Bacri, and G. Demouchy, Phys. Rev. E **65**, 031408 (2002).
[9] E. Blums, A. Mezulis, M. Maiorov, and G. Kronkalns, J. Magn. Magn. Mater. **169**, 220 (1997).
[10] E. Blums, S. Odenbach, A. Mezulis, and M. Maiorov, J. Magn. Magn. Mater. **201**, 268 (1999).
[11] E. Blums, J. Magn. Magn. Mater. **149**, 111 (1995).
[12] S. Odenbach, J. Magn. Magn. Mater. **149**, 116 (1995).
[13] J. Boussinesq, *Théorie Analytique de la Chaleur* (Gauthier-Villars, Paris, 1903), Vol. II, p. 172.
[14] J. K. Platten and G. Chavepeyer, Int. J. Heat Mass Transfer **19**, 27 (1976).
[15] H. R. Brand, P. C. Hohenberg, and V. Steinberg, Phys. Rev. A **30**, 2548 (1984).
[16] S. Hollinger, M. Lücke, and H. W. Müller, Phys. Rev. E **57**, 4250 (1998).
[17] A. La Porta and C. M. Surko, Phys. Rev. Lett. **80**, 3759 (1998).
[18] R. Cerbino, A. Vailati, and M. Giglio, Phys. Rev. E **66**, 055301(R) (2002).
[19] B. Huke, M. Lücke, P. Buchel, and C. Jung, J. Fluid Mech. **408**, 121 (2000).
[20] E. N. Lorenz, J. Atmos. Sci. **20**, 130 (1963).